MECHANICAL DESIGN ASPECTS OF THE LHC BEAM SCREEN

P. Cruikshank, K. Artoos, F. Bertinelli, J.-C. Brunet, R. Calder, C. Campedel, I. Collins, J.-M. Dalin, B. Feral, O. Grobner, N. Kos, A. Mathewson, L. Nikitina, I. Nikitine, A. Poncet, C. Reymermier, G. Schneider, I. Sexton, S. Sgobba, R. Valbuena, R. Veness,
CERN, Geneva, Switzerland.

Abstract

Forty-four kilometers of the LHC beam vacuum system [1,2] will be equipped with a perforated co-axial liner, the so-called beam screen. Operating between 5 K and 20 K, the beam screen reduces heat loads to the 1.9 K helium bath of the superconducting magnets and minimises dynamic vacuum effects. Constructed from low magnetic permeability stainless steel with a 50 μm inner layer of high purity copper, the beam screen must provide a maximum aperture for the beam whilst resisting the induced forces due to eddy currents at magnet quench. The mechanical engineering challenges are numerous, and include stringent requirements on geometry, material selection, manufacturing techniques and cleanliness. The industrial fabrication of these 16 metre long UHV components is now in its prototyping phase. A description of the beam screen is given, together with details of the experimental programme aimed at validating the design choices, and results of the first industrial prototypes.

1 INTRODUCTION

The LHC layout is defined by the existing 27 km LEP tunnel geometry. The two 7 TeV counter-rotating proton beams are separated horizontally in the arcs and channelled through twin-bore superconducting magnets. The two beam vacuum tubes, or cold bores, are the interface between the 1.9 K magnet baths of superfluid helium and the ultra high vacuum system. Synchrotron radiation power emitted by the proton beams (up to 0.32 W/m per beam), together with a comparable power dissipated by beam image currents, would represent an excessive heat load to the 1.9 K cryogenic system. In addition, an unacceptable gas density, and hence beam lifetime, would result from the dynamic equilibrium between cryopumped and desorbed (photon and ion induced) gas. The beam screen overcomes these problems by intercepting the heat loads at a higher and more thermo-dynamically efficient temperature. Also, by shielding the 1.9 K cryopumping surfaces from synchrotron radiation, gas in the beam aperture may be effectively cryopumped via holes (pumping slots) in the beam screen wall.

2 DESCRIPTION

The present design of the beam screen (Figure 1) is based on a 1 mm thick, ultra-low magnetic permeability stainless steel tube coated on its inner surface with a 50 μm layer of high electrical conductivity Cu. Two stainless steel cooling tubes, which maintain the beam screen temperature between 5 K and 20 K are positioned to optimise the available aperture [3]. A nominal annular gap of 1.5 mm between cold bore and beam screen is proposed to avoid thermal shorts and to accomodate the low thermal conductivity spring supports located at 1.7 metre intervals. Pumping slots on the flat zones of the beam screen body, representing some 4.4% of the inner surface area, have a randomised pattern which repeats every 500 mm ± 10 mm.

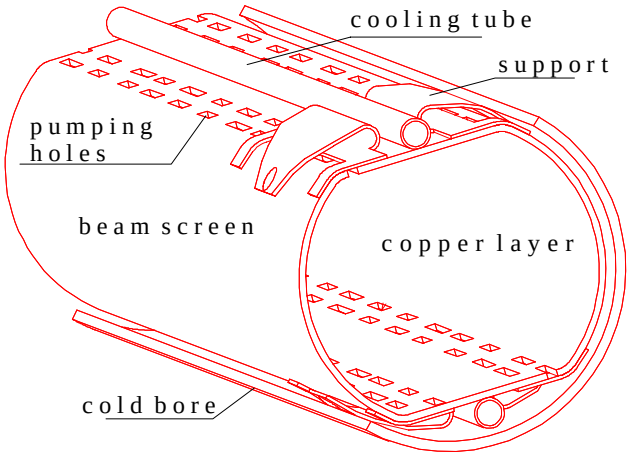

Figure: 1 The LHC beam screen

3 TECHNICAL REQUIREMENTS

3.1 Material Selection

To minimise resistive wall losses and coupling impedance, the inner surface of the beam screen must be of high electrical conductivity material [4]. High purity Cu with a relative resisitivity ratio (RRR) of approximately 100 is proposed. However, the large eddy current forces created during a magnet quench (section 3.2), imply that this Cu layer must be minimised and have excellent adherence to a high strength support structure, the beam screen body, which in turn must have an optimum thickness to maximise beam aperture. For the given geometry, it has been shown that a magnetic permeability of less than 1.005 (in the temperature range 5 K to 20 K) is required [5] to avoid significant magnetic field distortions. Conventional AISI 300 series stainless steels have permeabilities well in excess of this value.

0-7803-4376-X/98/$10.00 © 1998 IEEE

Several other vacuum compatible materials have been discounted due to their low temperature characteristics which show ferro-magnetic transitions (Ni superalloys - inconel, monel, etc.), fragility (titanium), or low strength (aluminium). Grades of austenitic stainless steel alloyed with Mn and Ni, having magnetic permeabilities < 1.005 at the operating temperature of the beam screen, such as Armco Nitronic 40, Ugine UNS 21904, Aubert & Duval X20MD are commercially available (typically 4 to 9% Mn, 7 to 10% Ni). However, laser welding trials have shown unacceptable levels of ferrite formation [6] due to nitrogen depletion in the weld bath. In collaboration with the steel industry, experimental batches of optimised higher alloyed grades (12% Mn, 11% Ni) have been produced and tested, showing excellent austenitic stability and ferrite free welds [7].

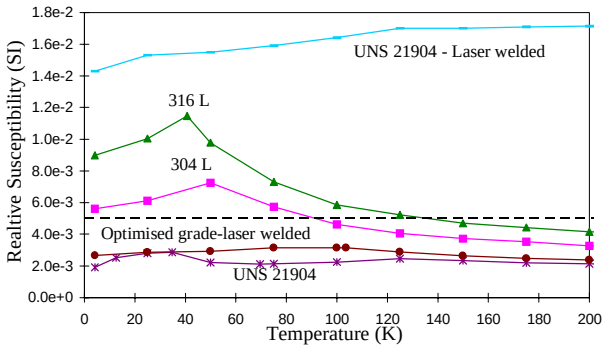

Figure: 2 Magnetic susceptibility of various stainless steels as a function of temperature.

3.2 Quench forces

A rapid decay of the 8.4 T magnetic field in the superconducting dipole magnets occurs during a resistive transition (quench) of the magnet windings. Large eddy currents are induced in the beam screen Cu layer, resulting in horizontal outward forces. The beam screen Cu layer must remain undamaged after repeated quenches. The maximum horizontal elastic deflection of the beam screen body must not exceed the annular gap between it and the cold bore, as the latter is simultaneously subjected to large external helium pressures [8]. Finite element quench calculations show good agreement with experimental beam screens (prior geometry with 304L stainless steel body) tested in 1 metre long model magnets [9,10]. Further testing of 11 metre beam screens in the LHC Prototype Half-Cell [11], together with the data from material testing will be used to optimise the stainless steel wall thickness.

3.3 Geometrical Tolerances

The manufacture tolerances specified for the beam screen x-section (0.2 mm), straightness (0.5mm/m) and twist between extremities (1°), are target values based upon manufacturing techniques and results of prototypes. Loss of beam aperture due to concentricity errors between cold bore and beam screen have been estimated [12].

3.4 Interconnections

Beam screens will be joined at magnet extremities by flexible RF sleeves which allow alignment and thermal contraction displacements. For security, helium to vacuum welds have been prohibited on the beam vacuum system and the seamless cooling tubes must traverse the cold bore envelope into the insulation vacuum at each magnet interconnect. Thermal transients imply that the cooling tubes must accept large movements (up to 44mm) with respect to the cold bore.

4 MANUFACTURE

The method of construction must consider the technical constraints as well as the necessity to economically produce 44 km of beam screen in lengths of 16 metres. For each step in the manufacturing process, many different techniques are possible. Figure 3 shows the methods of construction that have been retained.

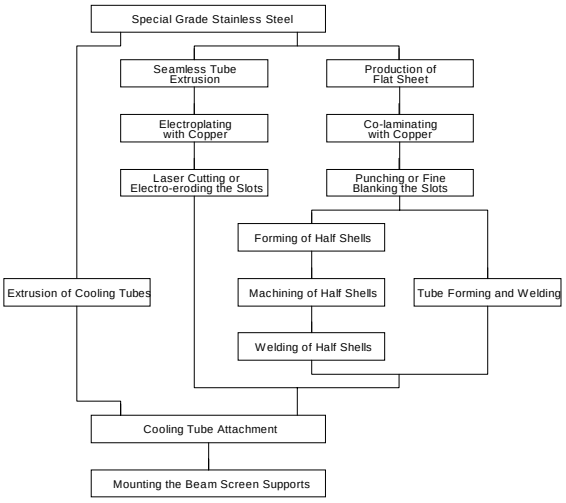

Figure: 3 Methods of construction

A key issue in the manufacturing process is the application of the Cu layer. It has been shown that prolonged heat treatment of electrodeposited Cu layers on stainless steel substrates above 550 °C will reduce the RRR to unacceptable values[13]. Therefore, once the Cu layer has been applied, high temperature brazing, welding with large heat input (TIG) or high temperature vacuum degassing are excluded from the manufacturing process, and extreme care is necessary to avoid mechanical damage or contamination of this soft Cu layer.

4.1 Attachment of the copper layer

Two methods are under investigation; electrodeposition and colamination (or roll-bonding). The former may be performed on both a closed geometry or a flat sheet.

4.1.1 Electroplating

Cu electroplating using a Ni strike increases the magnetic permeability of the beam screen; a 0.5 μm Ni layer

remains acceptable. Electrodeposited Cu layers on 1.2 metre beam screens have been characterised [14]. Eleven metre long prototype beam screens have been manufactured and installed at the Prototype Half-Cell.

4.1.2 Colamination

The colamination of stainless steel with Cu is obtained by cold rolling, followed by heat treatment to improve adhesion. First trials using UNS 21904 resulted in blistering of the Cu layer due to aluminium oxide contaminants at the stainless/Cu interface. Particles from the abrasive belts used to grind the stainless steel prior to colamination, had become embedded in the surface of the high strength alloy (R_m ~ 800 MPa). Subsequent trials have shown that the elimination of the grinding step produces acceptable colaminated material. During the heat treament cycle (which also moderates the steel properties) the RRR peaks at > 180 before decreasing sharply. Glow discharge optical spectroscopy has shown a diffusion of Mn into the Cu [15]. A compromise between Cu heat treatment (RRR ~ 60) and stainless steel annealing (R_p 0.2 ~ 600 MPa) is possible using a short heat treatment cycle (7.5 mins at 920 °C). The finished product shows excellent surface finish (Cu ; Ra < 0.2 μm) and thickness tolerances (Cu ; 50 ± 10 μm, St. Steel. ; 1.00 ± 0.02 mm). Further trials will be made with optimised stainless steel grades.

4.2 Beam screen body and cooling tubes

Production trials of seamless cooling tubes and beam screens in experimental grades of high manganese stainless steel have given acceptable results for the former, but failure for the latter due to high inclusion levels in the steel and the low ratio of wall thickness to diameter. Further tests using commercial grades are continuing. Sample beam screen bodies made from welded half shells have been manufactured in UNS 21904 (1.5 m) and AISI 316L (5.5 m). The technique of continuous tube forming from flat sheet may be applied for the beam screen body, and hence exploit the availabilty of colaminated material. Trials have been conducted using AISI 304L sheet, proving the feasibility for the beam screen geometry. The required geometrical tolerances (x-section, straightness, twist) go beyond the values obtained for industrially produced tubes. The use of sheet with good thickness tolerance, in-line laser welding and continous on-line dimensional control is expected to give improved results. Prototype beam screens of 16 metres length have been ordered in colaminated UNS 21904.

4.3 Pumping slots

Colaminated sheet can be on-line punched prior to forming. The narrow slot width (1.5 mm), high strength steel and limited lubrication choices (UHV compatibility) present challenges. Trial punching from the Cu side of colaminated sheet has shown fully ductile shearing with limited burr formation. For slot production on finished beam screen bodies, alternative methods (laser, laser with water jet, abrasive water jet, chemical etching, spark erosion) have also been evaluated [16].

4.4 Attachment of cooling tubes

Good thermal contact is required between the cooling tube and beam screen. Intermittent laser welding has been investigated (~ 500 spots/m), producing ferrite free welds with no measurable deformation to the beam screen body or visible damage to the Cu layer.

5 CONCLUSIONS

The LHC beam screen design continues to be optimised. Suitable materials have been developed and the joining techniques mastered. Progress has been made on each of the manufacturing techniques to be employed. Prototype 16 m beam screens have been ordered from industry.

6 REFERENCES

[1] The Large Hadron Collider, Conceptual Design, CERN, 95-05, October1995.

[2] O. Grobner, The LHC Vacuum System, PAC'97, Vancouver, Canada, May 1997.

[3] Y. Baconnier et al., LHC beam aperture and beam screen geometry, LHC Note 326, June 1995.

[4] F. Ruggiero et al., Surface resistance measurements for the LHC beam screen, PAC'97, Vancouver, Canada, May 1997.

[5] G. Houtappel, Multipoles in the magnets for LHC, caused by piping, air gap in yoke, cryostat, asymetric excitations and bus-bar currents, LHC-MMS, Internal Note 96-11, Sept. 1996.

[6] C. Boudot, S. Sgobba, Welding of Stainless Steels, International, Colloquium "Processing of Stainless Steels", Le Mons (B), 29-30 April 1997, page14-1ff.

[7] S. Sgobba, Techniques laser de soudage pour l'ecran de faisceau du grand collisioneur protonique (LHC), proceedings du Cycle Metaux et Procedes, Tremelan (CH), 4-8 Nov. 1996, vol. Journee soudage - page 8/1-10.

[8] M. Chorowshki et al., Thermohydraulics of resistive transitions on the LHC prototype magnet string: theoretical modelling and experimental results,-to be presented at CEC/ICMC 97, Portland, USA.

[9] K. Artoos et al., Mechanical and thermal measurements on a 1 m long beam screen. LHC Project Note 35, March 1996.

[10] R. Valbuena, Comparison de resultats de mesures realisees sur un ecran test et ceux donnes par le calcul, EST Technical Note EST-ESI 31/10/96, October 1996.

[11] R. Saban et al., Experiments and cycling at the LHC Prototype Half- Cell, PAC97, Vancouver, Canada, May 1997.

[12] N. Kos et al., Beam screen - cold bore concentricity, Vacuum Technical Note 96 - 24, December 1996.

[13] J.-M. Dalin, J. Hague, The effect of the temperature and duration of heat treatment on the electrical resistivity of electrodeposited copper, EST Internal Report MT-SM/93-06, April 1993.

[14] J.-M. Dalin, Caracterisation du depot de cuivre a l'interieur de l'ecran de faisceau du LHC, EST Internal Report EST-ESI 96-09-15, September 1996.

[15] Swiss Federal Laboratories for Materials Testing and Research EMPA, Test Report 165593, October 1996.

[16] G. Jesse, Examen metallurgique de differentes decoupes dans des toles inox avec une couche de cuivre colaminee pour l'ecran de faisceux LHC, EST Internal report, EST/MI/11/1/96, Jan. 1996.